Nuclear Engineering and Design 241 (2011) 1430–1437

Contents lists available at ScienceDirect

Nuclear Engineering and Design

journal homepage: www.elsevier.com/locate/nucengdes

Fluid-to-fluid modeling of two-phase flow critical heat flux in horizontal helically coiled tubes

Chang-Nian Chen[a], Ji-Tian Han[a,*], Tien-Chien Jen[b], Li Shao[a], Wen-Wen Chen[a]

[a] School of Energy and Power Engineering, Shandong University, No. 17923 Jingshi Rd., Jinan, Shandong Province 250061, PR China
[b] Department of Mechanical Engineering, University of Wisconsin-Milwaukee, Milwaukee, WI 53201, USA

ARTICLE INFO

Article history:
Received 2 June 2010
Received in revised form
17 December 2010
Accepted 29 December 2010

ABSTRACT

The new similarity laws for fluid-to-fluid modeling of two-phase flow critical heat flux (CHF) in horizontal helically coiled tubes were derived based on the dimensional analysis and similarity theory considering the effect of the geometrical parameters on CHF. A generalized factor D_n was introduced to the new similarity laws, and all the new dimensionless numbers were derived from the classical theorem of Buckingham π for dimensional analysis. The obtained dimensionless parameter sets were a reasonable extension to Ahmad's compensated distortion model, which may be considered as a special case of the new dimensionless parameter sets when the variable n is equal to unity. Based on the experimental data, the specific similarity numbers were determined for CHF phenomena in horizontal helically coiled tubes. A new equivalent characteristic parameter $D_{e\text{-}helix}$ was developed, which could reflect the influence of complex flow channels on the occurrence of CHF. The equivalent characteristic parameter consists of the essential geometrical parameters of tubes and the fluid thermophysical properties. The new fluid-to-fluid modeling methods were proposed for CHF of R134a-water in horizontal helically coiled tubes, which could be used readily to derive the CHF data of water through the CHF data of R134a at the corresponding experimental conditions.

1. Introduction

Critical heat flux (CHF) is very important for reliable design and safe operation of boiling heat transfer facilities. Investigations on CHF are usually conducted with experiments due to the complicated mechanism of CHF phenomena. However, experimental study of CHF in water must be performed under high pressure and high temperature conditions that require a very complicated experimental system, very high heating power and very careful operation, resulting in more difficulties and expenditures in experimentation (Collier and Thome, 1996). Nevertheless, some low latent heat substances such as Freon can be used as working fluid in CHF experiments with low pressure and low temperature, which significantly reduces the difficulties mentioned above in water. Fluid-to-fluid modeling of CHF is a method to deduce CHF data in modeling fluid such as Freon under low pressure and temperature to data of prototype fluid, such as water, based on the dimensionless similar relationship.

Fluid-to-fluid modeling technique of CHF is considered to be the precursor to modeling experiments. Barnett (1963, 1964) and Barnett and Wood (1965) first developed modeling scaling laws for CHF using low latent heat substance Arcton-12 and Freon-12 etc. They deduced a new method of approach to dimensionless equations and tested its validity. Subsequently, many models were proposed successfully by equation-analysis or dimensionless-analysis methods. Stevens and Kirby (1964) carried out the fundamental work for fluid-to-fluid modeling and developed their modeling method, with comparing CHF data in water at 6.90 MPa with CHF data in R12 at 1.07 MPa in vertical round tubes. Afterward, Fulfs (1980) also evaluated and confirmed its validity for use on reactor bundles. In addition, they discussed the restriction on the size for modeling technique using R12 to model forced convection burnout CHF in water (Stevens and Macbeth, 1970). Actually, the geometric size of model has a significant effect on fluid-to-fluid modeling method, especially for complex flow channels. Dix (1970) performed Freon–water fluid modeling of CHF in round tubes, and he found that the mass flux modeling factor was influenced by the combination function of pressure, mass flux and length-to-diameter ratio. Groeneveld (1970) developed the similarity laws for water and Freon according to dryout data in uniformly heated tubes, mainly concerning the improving of mass flux modeling factor. Ahmad (1973) brought forward his famous theory in fluid to fluid modeling method: the compensated distortion model, and he proposed a combined dimensionless modeling

* Corresponding author. Tel.: +86 53188399060; fax: +86 53188399060.
E-mail address: jthan@sdu.edu.cn (J.-T. Han).

0029-5493/$ – see front matter © 2011 Elsevier B.V. All rights reserved.
doi:10.1016/j.nucengdes.2010.12.021

Nomenclature

a, b, c	empirical constants
a_i	the ith exponential in Eq. (5)
C_p	specific heat capacity, kJ kg^{-1} K^{-1}
D	hydraulic diameter, m
D_c	coil diameter, m
$D_{e\text{-}helix}$	characteristic length parameter defined in Eq. (11)
D_n	generalized factor, m
d_i	inner diameter of the test tube, m
G	mass flux, kg m^{-2} s^{-1}
g	gravitational acceleration, m s^{-2}
K	thermal conductivity, W m^{-1} K^{-1}
L	length or valid heated length, m
n	variable
P_t	helical pitch, m
q_c	critical heat flux, kW m^{-2}
S	section symbol of the test tube

Greek symbols

ΔH	subcooling enthalpy, J kg^{-1}
Ψ_{CHF}	modeling parameter
ψ'_{CHF}	new modeling parameter
α_i	the ith geometric parameters of a specific configuration in Eq. (3)
β	defined as $\left\lvert \frac{\partial(\theta)}{\partial P} \right\rvert_{\text{saturation}}$
γ	defined as $\left\lvert \frac{\partial(\rho_l/\rho_g)}{\partial P} \right\rvert_{\text{saturation}}$
λ	latent heat of evaporation, J kg^{-1}
μ	dynamic viscosity, Pa s
π_i	the ith dimensionless product derived by dimensionless analysis
ρ	density, kg m^{-3}
σ	surface tension, N m^{-1}

Subscripts

g	gas phase
l	liquid phase
M	modeling fluid
P	prototype fluid

parameter including liquid Reynolds number, Weber number and gas Reynolds number. This compensated distortion model can be extensively applied to CFCs, CO_2 and potassium in straight round tubes and bundles. Katto (1978) established his modeling method for water and R12, which was essentially consentaneous with Ahmad's model. Moreover, his new dimensionless parameter was more compact and simple to use for calculating mass flux modeling factor. Merilo (1979) conducted a study on fluid-to-fluid modeling CHF of water-R12 in horizontal tubes based on compensated distortion model. The modeling parameter obtained by Merilo differed from the one applicable to vertical flow due to the additional effects of gravity. In his study, the mass flux scaling factor for modeling water with R12 in horizontal flow was generally higher than that for vertical flow, and it showed a greater sensitivity to pressure. Green and Lawther (1981) developed CHF correlations for water and R12 in boiling flow. His correlation was based on parameter groups derived from dimensional analysis and had been compared with experimental CHF data for R12 and for water with the RMS errors of 3.3% and 5.8%, respectively. Zhang (1984) and Lu et al. (1988) suggested a set of new dimensionless numbers, which promotes Ahmad's model. Their innovation in refining the modeling method was to replace the gas-phase Reynolds number in Ahmad model with the gas-phase Prandtl number. Chen et al. (2003, 2004) performed CHF experiments and fluid-to-fluid modeling studies in round tubes and bundles for reactor applications. They determined that the Ahmad compensation distortion model (Ahmad, 1973), the Lu model (Lu et al., 1988), the Groeneveld model (Groeneveld, 1970) and the Stevens–Kirby model (Stevens and Kirby, 1964) all overpredicted the bundles CHF values for water and proposed a new empirical correlation for calculating mass flux scaling factor.

On the other hand, the CFCs substances such as R11, R12 and R22 have a destructive influence on the ozonosphere. Due to the limitation imposed by the Montreal Protocol for CFCs, alternative refrigerants such as R134a, which are harmless to ozonosphere and have excellent thermophysical properties of low pressure, low temperature, and low vaporization heat, have been considered as promising modeling fluids (Groeneveld et al., 1997; Tain et al., 1993; Thome, 1994).

Reviewing of the previous efforts, most of the CHF modeling techniques were used in straight round tubes or bundles, and the outgoing CFCs substances were usually used as modeling fluids. Studies on fluid-to-fluid modeling methods of CHF in complex flow channels such as helically coiled tubes are scarce. Moreover, the modeling experiments were usually carried out using the same model as the prototype in geometric size. Thus, the effect of geometric parameters on the characteristics of flow boiling has been ignored. Actually, the complicated geometric parameters have significant influence on flow boiling heat transfer (Han et al., 2004; Pioro et al., 1999; Xin et al., 2001; Yang et al., 2005). To take this influence on CHF into account, this paper introduced a generalized factor D_n to the fluid-to-fluid modeling method. Thirteen similar dimensionless products were derived based on the dimensional analysis and similarity theory. New fluid-to-fluid modeling methods were proposed for CHF of R134a-water in horizontal helically coiled tubes.

2. Theoretical analysis

2.1. Extension to principle of similarity

Because the CHF phenomena are too complicated to be described in a mathematical equation accurately, the most effective way to study it is to use the dimension analysis method to find out the relationship among all the main variables. As a typical method for fluid-to-fluid modeling, Ahmad's compensated distortion model (Ahmad, 1973) has been widely used in practice. Ahmad summarized the generalized relationship among main variables in flow boiling heat transfer as follows:

$$f(q_c, G, \Delta H, L, D, g, \lambda, \rho_l, \rho_g, \mu_l, \mu_g, C_{P_l}, C_{P_g}, K_l, K_g, \sigma, \gamma, \beta) = 0 \quad (1)$$

Thirteen dimensionless products were derived by Ahmad based on Eq. (1). For a complete modeling description, it is necessary to ensure that all the dimensionless groups are identical for both model and prototype according to similarity theory (Langhaar, 1967; Sun, 1979). However, for more complex flow channels, it is difficult to satisfy such a requirement. Furthermore, the incomplete model for modeling appears to be distorted. To compensate this distortion, Ahmad (1973) proposed the following dimensionless groups for CHF analysis:

$$\frac{q_c}{G\lambda} = f\left(\psi_{CHF}, \frac{\Delta H}{\lambda}, \frac{\rho_l}{\rho_g}, \frac{L}{D}\right), \qquad \psi_{CHF} = \left[\frac{GD}{\mu_l} \cdot \left(\frac{\gamma^{1/2}\mu_l}{D\rho_l^{1/2}}\right)^{2/3} \cdot \left(\frac{\mu_l}{\mu_g}\right)^{1/8}\right] \quad (2)$$

Nevertheless, this compensated distortion model just takes L and D into account for geometric number group, not including other significant geometrical parameters for specific configuration such as coil diameter and helical pitch (helical angle) in a helically coiled tube. Considering the effect of complex geometrical parameters on

Table 1
Comparison of the new results with reference (Ahmad, 1973).

No.	Dimensionless numbers	Results of reference (Ahmad, 1973)	New results
1	Boiling number	$\pi_1 = \frac{q_c}{G\lambda}$	$\pi_1 = \frac{q_c}{G\lambda}$
2	Reynolds number	$\pi_2 = \frac{GD}{\mu_l}$	$\pi_2 = \frac{GD_n}{\mu_l(\sigma\gamma)^{n-1}}$
3	Weber–Reynolds number	$\pi_3 = \frac{\mu_l{}^2}{\sigma D\rho_l}$	$\pi_3 = \frac{\mu_l{}^2(\sigma\gamma)^{n-1}}{\sigma D_n\rho_l}$
4	Liquid-to-gas viscosity ratio	$\pi_4 = \frac{\mu_l}{\mu_g}$	$\pi_4 = \frac{\mu_l}{\mu_g}$
5	Subcooling number	$\pi_5 = \frac{\Delta H}{\lambda}$	$\pi_5 = \frac{\Delta H}{\lambda}$
6	Liquid-to-gas density ratio	$\pi_6 = \frac{\rho_l}{\rho_g}$	$\pi_6 = \frac{\rho_l}{\rho_g}$
7	Geometric number	$\pi_7 = \frac{L}{D}$	$\pi_7 = \frac{L^n}{D_n}$
8	Froude–Reynolds number	$\pi_8 = \frac{gD^3\rho_l{}^2}{\mu_l{}^2}$	$\pi_8 = \frac{gD_n{}^3\rho_l{}^2}{\mu_l{}^2(\sigma^3\gamma^3)^{n-1}}$
9	Liquid Prandtl number	$\pi_9 = \frac{\mu_l C_{P_l}}{K_l}$	$\pi_9 = \frac{\mu_l C_{P_l}}{K_l}$
10	Gas Prandtl number	$\pi_{10} = \frac{\mu_g C_{P_g}}{K_g}$	$\pi_{10} = \frac{\mu_g C_{P_g}}{K_g}$
11	Liquid-to-gas thermal conductivity ratio	$\pi_{11} = \frac{K_l}{K_g}$	$\pi_{11} = \frac{K_l}{K_g}$
12	Barnett number	$\pi_{12} = \frac{\gamma^{1/2}\mu_l}{D\rho_l{}^{1/2}}$	$\pi_{12} = \frac{\gamma^{1/2}\mu_l(\sigma\gamma)^{n-1}}{D_n\rho_l{}^{1/2}}$
13	Saturation temperature number	$\pi_{13} = \frac{C_{P_l}\beta}{\lambda\gamma}$	$\pi_{13} = \frac{C_{P_l}\beta}{\lambda\gamma}$

boiling heat transfer, especially for CHF phenomena, a generalized factor is used to replace the hydraulic diameter D in Eq. (1). D_n is defined as follows:

$$D_n = f(\alpha_1, \alpha_2, \ldots, \alpha_m) \tag{3}$$

According to the knowledge of heat and mass transfer and hydrodynamics, it is appropriate to select such five fundamental dimensions as M, L, T, θ, H for analysis. They represent mass, length, time, temperature and quantity of heat, respectively. One can set the dimension of D_n as L^n, which is comprehensible from its physical meanings. So Eq. (1) can be transformed to Eq. (4) based on the above hypothesis:

$$f(q_c, G, \Delta H, L, D_n, g, \lambda, \rho_l, \rho_g, \mu_l, \mu_g, C_{P_l}, C_{P_g}, K_l, K_g, \sigma, \gamma, \beta) = 0 \tag{4}$$

The six groups, $\Delta H/\lambda$, L^n/D_n, ρ_g/ρ_l, μ_g/μ_l, C_{P_g}/C_{P_l} and K_g/K_l are dimensionless evidently. And the other dimensionless products can be described as the form of exponent:

$$\pi_i = q_c^{a_1} G^{a_2} D_n^{a_3} g^{a_4} \lambda^{a_5} \rho_l{}^{a_6} \mu_l{}^{a_7} C_{P_l}^{a_8} K_l^{a_9} \sigma^{a_{10}} \gamma^{a_{11}} \beta^{a_{12}} \tag{5}$$

Then, a dimensionless matrix is derived from Eq. (5) as follows:

	a_1	a_2	a_3	a_4	a_5	a_6	a_7	a_8	a_9	a_{10}	a_{11}	a_{12}
	q_c	G	D_n	g	λ	ρ_l	μ_l	C_{P_l}	K_l	σ	γ	β
M	0	1	0	0	−1	1	1	−1	0	1	−1	−1
L	−2	−2	n	1	0	−3	−1	0	−1	0	1	1
T	−1	−1	0	−2	0	0	−1	0	−1	−2	2	2
θ	0	0	0	0	0	0	0	−1	−1	0	0	1
H	1	0	0	0	1	0	0	1	1	0	0	0

(6)

Consequently, the remnant dimensionless products can be calculated by the matrix method for solving principle of similarity (Langhaar, 1967; Sun, 1979). Seven new dimensionless products with variable n are derived, and there are also in total of thirteen including the six mentioned above. They are listed in Table 1 as well as the results of Ahmad for comparison.

2.2. Modeling method and discussion

From the comparison of data in Table 1, it is determined that the difference between the new results and Ahmad's is that variable n has been included in most of the new similarity numbers. It is also noted that if the variable n is equal to unity (the dimension of D_n is L), Ahmad's results are identical to the new ones. In this situation:

$$D_n = D_1 = D \tag{7}$$

As a result, Ahmad's results may be considered as a special case of the new dimensionless parameter sets when the variable n is equal to unity.

The construction of new fluid-to-fluid modeling method obeyed the same principles as Ahmad (1973) did. The main similarity numbers were selected according to their roles played in the CHF conditions and the correlations used to associate experimental results with scaling analysis were formed by both of equations and single-valued conditions. New dimensionless groups for CHF analysis selected here are as follows:

$$\frac{q_c}{G\lambda} = f\left(\psi'_{CHF}, \frac{\Delta H}{\lambda}, \frac{\rho_l}{\rho_g}, \frac{L^n}{D_n}\right) \tag{8}$$

where ψ'_{CHF} is the new compound parameter for new modeling method. It is a function of Reynolds number, Weber–Reynolds number and Liquid-to-gas viscosity ratio.

$$\psi'_{CHF} = \left[\left(\frac{GD_n}{\mu_l(\sigma\gamma)^{n-1}}\right)^a \cdot \left(\frac{\mu_l{}^2(\sigma\gamma)^{n-1}}{\sigma D_n\rho_l}\right)^b \cdot \left(\frac{\mu_l}{\mu_g}\right)^c\right] \tag{9}$$

where constants n, a, b and c can be determined by experimental data.

For the purpose of fluid-to-fluid modeling of R134-water in horizontal helically coiled tubes, it is most important to obtain the specific form of D_n. As mentioned above, D_n is a compound geometric parameter. It must represent the main characteristics of one specific flow channel well and truly. For horizontal helically coiled tubes, geometrical parameters such as coil diameter D_c, valid heated length L, tube inner diameter d_i and helical pitch P_t have a significant effect on CHF due to the conjunct function of gravity and centrifugal force on fluid flow and heat transfer. Therefore, the following form of D_n is tentatively suggested according to the analysis of experimental data:

$$D_n = f(D_c, L, d_i, Pt) = L^n + \left(\frac{D_c}{d_i} \cdot Pt\right)^n + \left(\frac{d_i}{L} \cdot Pt\right)^n \tag{10}$$

For further understanding, the meanings for introducing the generalized factor D_n can be explained as follows. Comparing the new dimensionless products with Ahmad's, it is noted that a new equivalent characteristic parameter $D_{e\text{-}helix}$ has been defined as below:

$$D_{e-helix} = \frac{D_n}{(\sigma\gamma)^{n-1}} \tag{11}$$

The dimension of this characteristic parameter $D_{e\text{-}helix}$ is L, which is identical to that of the general length characteristic parameter. It consists of the essential geometric parameters of horizontal helically coiled tubes such as coil diameter, valid heated length, tube inner diameter, helical pitch and the fluid thermophysical properties such as the surface tension σ and the compound parameter γ related to density ratio of liquid–vapor two phase. It is known that surface tension will restrain the liquid film from being dispersed. The variation of density ratios of liquid–gas will determine whether Taylor stability could be kept or Helmholtz stability would be lost, which supports the explanation for the departure from nucleate boiling (DNB) or dry-out mechanism for CHF to some extent.

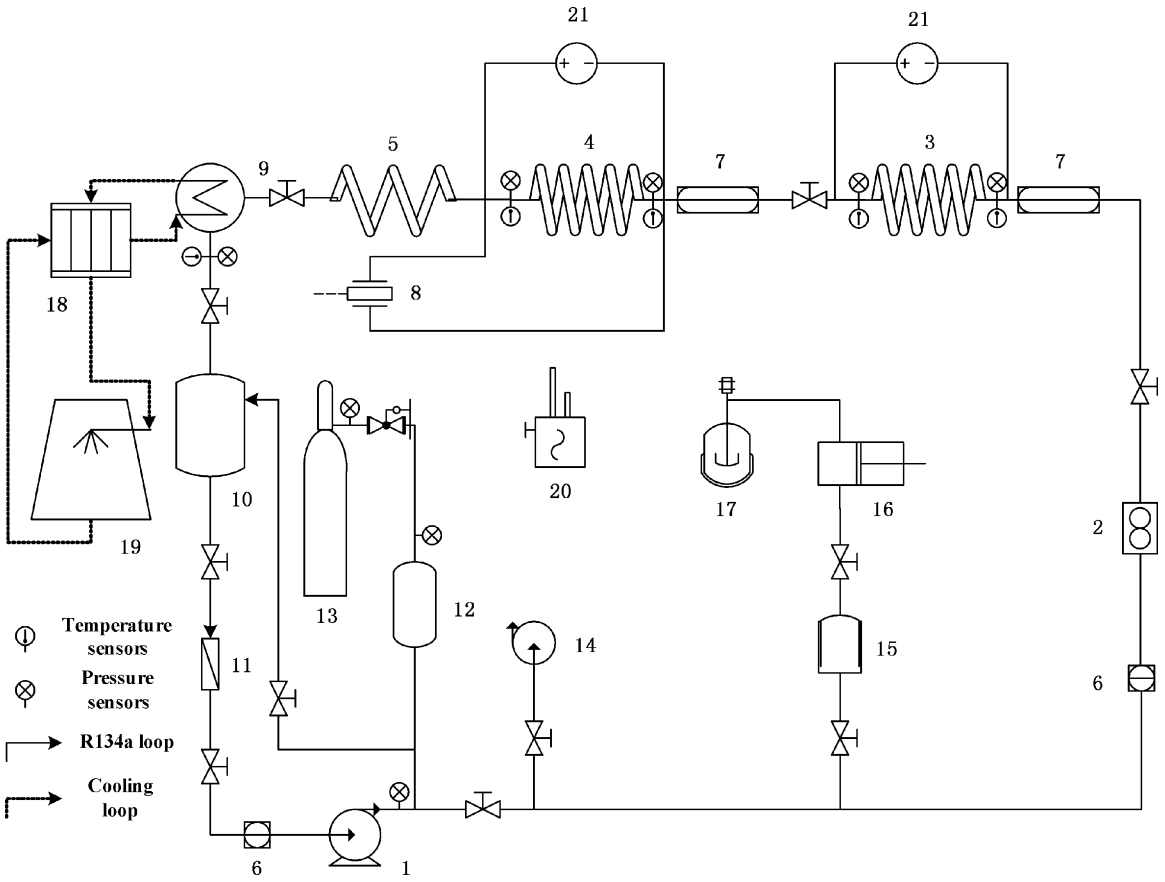

Fig. 1. Schematic diagram of the experimental circle loop. 1 Motor pump, 2 coriolis mass flowmeter, 3 preheated section, 4 test section, 5 flow pattern observing section, 6 sight glass, 7 visual section, 8 differential pressure gage, 9 condenser, 10 receiver tank, 11 dry-strainer, 12 accumulator, 13 N_2 gas tank, 14 vacuum pump, 15 buffer tank, 16 refrigerant pump, 17 refrigerant tank, 18 chilling unit, 19 cooling tower, 20 halogens leak detector, 21 DC power supply.

3. Experiments and fluid-to-fluid modeling results

3.1. Experiments

In order to obtain CHF data for water in horizontal helically coiled tubes with modeling fluid R134a, experiments were carried out in a R134a test loop, as shown in Fig. 1. It includes the following components: canned motor pump (1), coriolis mass flowmeter (2), preheating section (3), test section (4), precision DC power supplies (21), condenser (9), refrigeration chilling unit (18), N_2-gas accumulator (12) and data acquisition system. This experimental set-up is designed for pressure of 1.6 MPa and temperature of 200 °C, preheated section power supply of 24 V × 300 A and test section power supply of 60 V × 500 A. The refrigeration chilling unit has a maximum output of 50 kW.

Three test sections made of stainless steel tubes (SUS304) were directly and uniformly heated by high current DC power supplies. The ranges of experimental condition are shown in Table 2.

The temperatures in R134a bulk flow are measured by 0.3 mm T-type sheathed thermocouples. The precision pressure sensors are set at the same positions as thermocouples in order to measure the local pressures. The temperatures of outside wall are measured by 0.2 mm T-type thermocouples set along the test tube. Eight symmetrical positions of each coil of the helically coiled tube as s1–s8 indicated in Fig. 2, are selected as measuring sections where four thermocouples are set evenly around the circumferences, as T1–T4 indicated in Fig. 2. The test tubes are wrapped by PEF (polyethylene chemical bridging highly foamed materials) for heat preservation, since it has a heat loss less than 5%. All the experimental signals are transmitted to Agilent 34980A data acquisition system for processing.

R134a from the receiver tank is circulated through the whole system by canned motor pump. The mass flux can be controlled by adjusting the speed of pump motor and control valves. The pressure is controlled by adjusting mass flux of cooling loop, power supply of preheated section and N_2-gas accumulator. When the pressure and mass flux of the system are stabilized to predetermined values, the inlet temperature is controlled by increasing or decreasing power supply to preheated section. The power supply to test section is increased rapidly at the beginning, then slowly at each step of about 0.05 kW m^{-2} until CHF occurs. A method based on the event-driven Agilent BenchLink Data Logger Pro software was developed to determine the occurrence of CHF. Once the wall temperature reaches the limited value set in advance, the Agilent software alerts the operator shuts off power supplies within 0.1 s.

Based on the instructions from experiment equipment and verified data sheet, the maximum uncertainty in measuring length and inner diameter of test section is ±0.093% and ±0.53%, respectively; the maximum uncertainty in measuring temperature is ±0.45%; the maximum uncertainty in measuring pressure is ±2.6%; the maximum uncertainty in measuring mass flux is ±2.1%; the maximum uncertainty in measuring voltage and current is ±2% and ±1.7%, respectively. Therefore, the maximum uncertainty in measuring the heated area of test tube and critical heat flux value is about ±0.54% and ±2.7%, respectively, according to Moffat's experimental error transfer procedure (Moffat, 1988).

Table 2
Experimental condition ranges for CHF in R134a.

Test sections	Geometrical parameters (mm)					Pressure (MPa)	Mass flux (kg m^{-2} s^{-1})	Inlet quality	Heat flux (kW m^{-2})
	d_o	d_i	D_c	L	P_t				
Tube 1	6	3.8	300	1886	45	0.15–0.55	60–550	−0.35–0.33	6–90
Tube 2	10	7.6	170	1073	45				
Tube 3	10	8.4	300	1890	75				

3.2. Discussion and comparison with existing CHF data in water

In order to investigate the characteristics of CHF phenomenon in helically coiled tubes, more CHF experiments were conducted to analysis the wall temperature distribution, the effect of system flow parameters on CHF value with experimental conditions of pressures of 0.2–1.35 MPa, mass fluxes of 50–400 kg m^{-2} s^{-1}, inlet qualities of −0.15–0.35 and heat fluxes of 12–38.5 kW m^{-2}.

All the experiments were performed with medium mass flux and low pressure conditions, and for data reduction, critical heat flux q_{cr} is calculated by Eq. (12). The inlet and outlet vapor qualities x_i and x_o are evaluated by Eq. (13) based on energy balance. The local vapor quality x_l is determined by Eq. (14).

$$q_{cr} = \frac{U \cdot I}{A_e} \tag{12}$$

$$x_i = \frac{\Delta i_2 + \Delta i_1 - \Delta i_0}{\gamma}, \qquad x_o = x_i + \frac{\Delta i_e}{\gamma} \tag{13}$$

$$i_l = i_i + \Delta i_l, \qquad x_l = f(i_l, P_l) \tag{14}$$

where i_i and Δ_{i_l} are the enthalpy of R134a at the inlet and the enthalpy increase from the inlet to the local section of the test tube, respectively. The local pressure P_l can be obtained by linearly interpolating the readings of pressure transducers set in the inlet and outlet of test section.

Under current experimental conditions, most of the CHF results belong to dry-out type CHF according to the classical critical heat flux theory (Collier and Thome, 1996; Lu, 2002). It usually occurs in the nearest section of test tube outlet and spreads to the front sections immediately; the wall temperature will then increase very quickly up to 3–4 times, as shown in Fig. 3(a). Though it is difficult to distinguish the exact position from which CHF starts, the wall temperatures at the fronts and offsides (T2 and T4) of one section frequently are much higher than the other two sides. And the wall temperatures of S1 rise much earlier than those of S2 as shown in Fig. 3(a). On the other hand, the abrupt rise of the section temperature along the heated length of tube with local vapor qualities also suggests the occurrence of CHF, as shown in Fig. 3(b). It is noted that the section temperature always jumps near the outlet with an average temperature difference of about 20 °C.

The CHF values have an approximately linear increasing trend with mass fluxes and it seems like that this trend slightly moves up at lower inlet vapor qualities, as shown in Fig. 4(a). It is also noted that CHF values decrease linearly with increasing inlet vapor qualities according to the fact that the decline gradients of δq_{cr} are nearly the same among different inlet vapor qualities, as shown in Fig. 4(a). Besides, the outlet pressure has less effect on CHF than mass flux and inlet vapor quality, and the CHF value decreases a little with pressure increasing. The CHF values decrease with outlet vapor qualities increasing, as shown in Fig. 4(b). It also shows that the vapor qualities at higher mass fluxes are lower than those at lower mass fluxes, while CHF values vary more smoothly with vapor qualities at lower mass fluxes. System pressure has little effect on CHF value under most of the experimental conditions.

With the analysis of R134a CHF data in horizontal helically coiled tubes, the constants n, a, b and c in Eq. (9) were determined as follows:

(1) Considering the independence of the constants a, b and c, it will be simplified for calculation supposing the constant $a = 1$, thus Eq. (9) will be:

$$\psi'_{CHF} = \left[\left(\frac{GD_n}{\mu_l(\sigma\gamma)^{n-1}} \right) \cdot \left(\frac{\mu_l{}^2(\sigma\gamma)^{n-1}}{\sigma D_n \rho_l} \right)^b \cdot \left(\frac{\mu_l}{\mu_g} \right)^c \right] \tag{15}$$

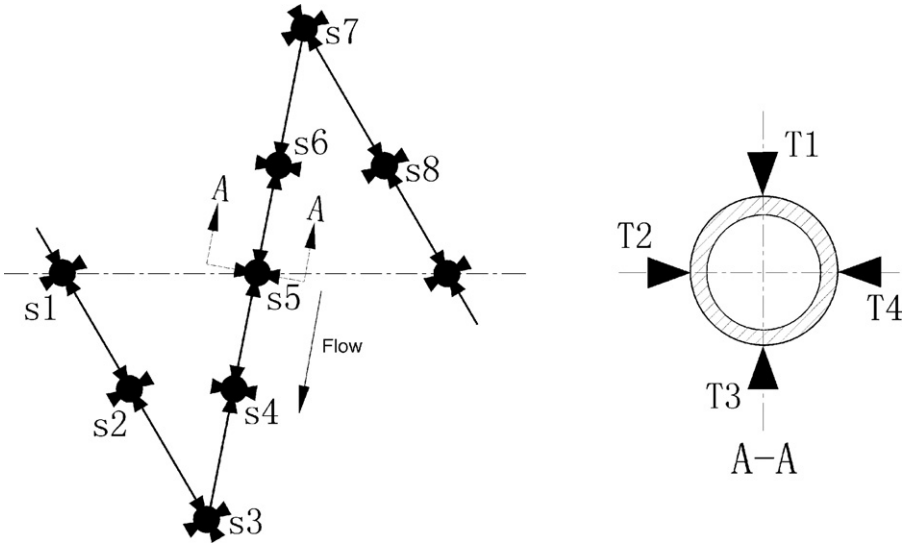

Fig. 2. Schematic diagram of the installation of thermocouples.

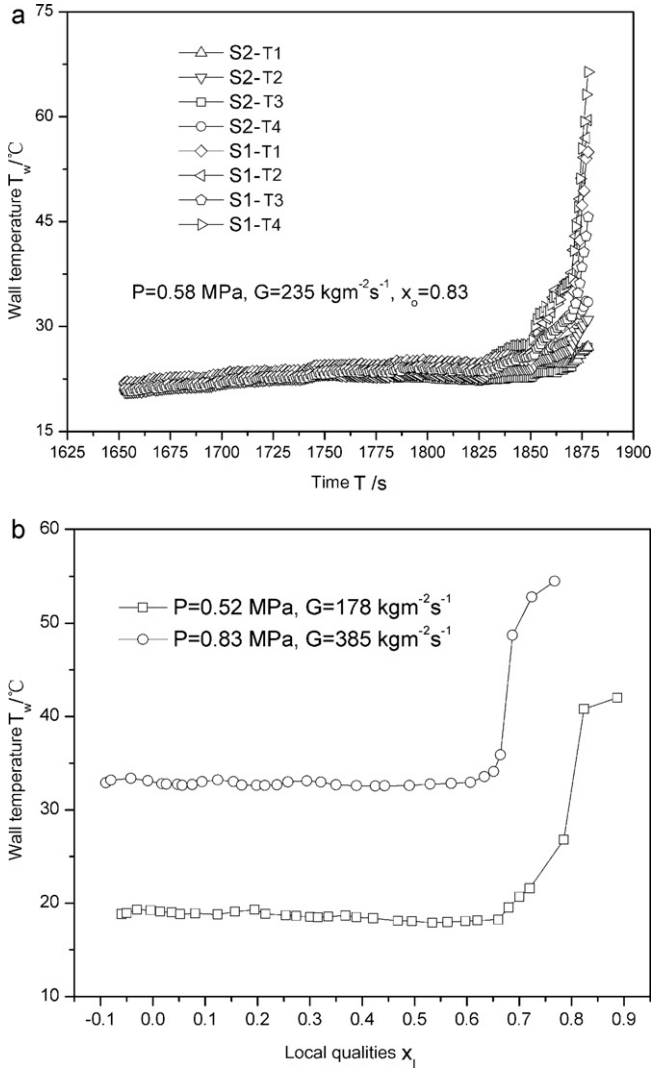

Fig. 3. (a) Wall temperature distribution when CHF occurs. (b) Wall temperature distribution with local vapor qualities.

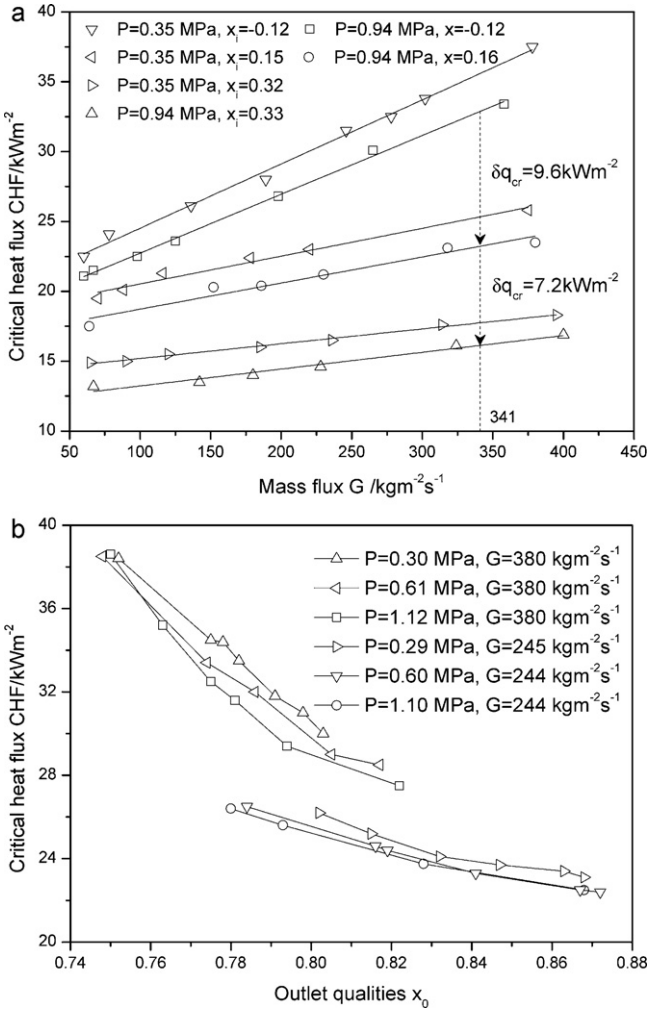

Fig. 4. (a) Effect of mass flux and inlet quality on CHF. (b) Effect of outlet quality on CHF.

(2) Since there are only three constants b, c and n in the above equations and all the experimental results under different conditions should obey the same relationship in Eq. (8), three and more experiments with different system conditions can be used to determine the values of all the constants for certain specific test section.
(3) b, c and n should be optimized according to experimental data for different test sections with different geometrical parameters. A generalized n should be determined firstly for all the geometrical parameters, and then b and c are calculated based on the determined value of n.

According to the calculation steps mentioned above, it was found that there was a satisfying result when $n = 1.62$, $a = 1$, $b = 0.38$ and $c = 0.14$. Hereafter, the new modeling method has got into shape and the following equations should be satisfied at the same time.

$$(\psi'_{CHF})_P = (\psi'_{CHF})_M, \qquad \left(\frac{\Delta H}{\lambda}\right)_P = \left(\frac{\Delta H}{\lambda}\right)_M,$$
$$\left(\frac{\rho_l}{\rho_g}\right)_P = \left(\frac{\rho_l}{\rho_g}\right)_M, \qquad \left(\frac{L^n}{D_n}\right)_P = \left(\frac{L^n}{D_n}\right)_M \tag{16}$$

The validity of the new fluid-to-fluid modeling method was confirmed by comparing the CHF data translated from R134a experiments in horizontal helically coiled tubes with existing CHF data in water derived by Hou (2000), whose experimental condition ranges are listed in Table 3. The selected condition ranges

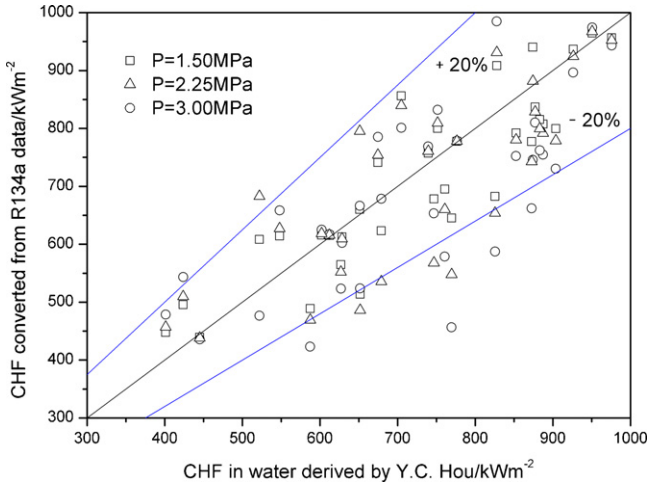

Fig. 5. Comparison CHF converted from R134a with existing data in water.

Table 3
Experimental condition ranges for CHF in water (Hou, 2000).

Test sections	Geometrical parameters (mm)					Pressure (MPa)	Mass flux ($kg\,m^{-2}\,s^{-1}$)	Inlet subcooled temperature (°C)	Heat flux ($kW\,m^{-2}$)
	d_o	d_i	D_c	L	P_t				
Tube 1	8	6	64	2211	25	0.75–3.00	150–910	40–50	0–850
Tube 2	10	7	103	1838	25				
Tube 3	12	9	305	1437	35				

Table 4
Selected conditions in R134a and the corresponding conditions in water.

Pressure (MPa)		Saturated temperature (°C)		Mass flux ($kg\,h^{-1}$)	
R134a	Water	R134a	Water	R134a	Water
0.23	1.50	−6.5	198.3	37.0, 49.3, 61.6, 74.0	54, 72, 90, 108
0.35	2.25	5.0	218.5	37.4, 49.8, 62.3, 74.7	
0.47	3.00	13.8	233.9	37.5, 50.0, 62.5, 75.0	

in R134a for comparison with CHF data in water are shown in Table 4.

Fig. 5 shows the comparison results with pressures of 1.50, 2.25, 3.00 MPa and mass fluxes of 54, 72, 90, 108 $kg\,h^{-1}$ in water. A good agreement is achieved between the converted CHF data from R134a using new fluid-to-fluid modeling method for horizontal helically coiled tubes and the existing CHF data in water, with an error of 20% as indicated in Fig. 5.

4. Conclusions

A study of fluid-to-fluid modeling of CHF of R134a-water in horizontal helically coiled tubes was conducted in this paper. Considering the effect of complex geometric parameters on flow boiling CHF, introducing a generalized factor D_n and proposing a new fluid-to-fluid modeling method was developed for practical and immediate applications.

(1) A group of new dimensionless products for fluid-to-fluid modeling of CHF were derived according to the dimensional analysis and similarity theory. Ahmad's results for compensated distortion model may be considered as a special case of the new results when the variable n is equal to unity.
(2) A new equivalent characteristic parameter, $D_{e\text{-}helix}$, was developed, which is a combination of the essential geometric parameters and the fluid thermophysical properties and can reflect the influence of complex flow channels on the occurrence of CHF. It is consistent with the purpose of introduction of the generalized factor D_n.
(3) Compared with existing CHF data in water, the new fluid-to-fluid modeling method proposed in this paper gives a satisfactory result with an error of ±20% in the ranges of selected experimental conditions.

Acknowledgements

This work was supported by The National Natural Science Foundation of China (No. 50776055 and No. 51076084). Dr. Tien-Chien Jen would also like to acknowledge partial financial support from EPA (USA) award RD 833357.

References

Ahmad, S.Y., 1973. Fluid to fluid modeling of critical heat flux: a compensated distortion model. Int. J. Heat Mass Trans. 16, 641–662.
Barnett, P.G., 1963. The scaling of forced convection boiling heat transfer. U.K.A.E.A. Report, Winfrith, Dorset, England, AEEW-R134.
Barnett, P.G., 1964. An experimental investigation to determine the scaling laws of forced convection boiling heat transfer. Part 1: the preliminary examination of burnout data for water and Arcton 12. U.K.A.E.A. Report, Winfrith, England, AEEW-R363.
Barnett, P.G., Wood, R.W., 1965. An experimental investigation to determine the scaling laws of forced convection boiling heat transfer. Part 2: an examination of burnout data for water, Freon 12 and Freon 21 in uniformly heated round tubes. U.K.A.E.A. Report, Winfrith, England, AEEW-R443.
Collier, J.G., Thome, J.R., 1996. Convective Boiling and Condensation, 3rd ed. Claredon Press, Oxford, England.
Chen, J., Yang, Y.H., Liao, J.R., Zhao, H., 2003. Fluid to fluid modeling of CHF in round tube. Nucl. Power Eng. 24, 354–358.
Chen, J., Liao, J.R., Kuang, B., Zhao, H., Yang, Y.H., 2004. Fluid-to-fluid modeling of critical heat flux in 4 × 4 rod bundles. Nucl. Eng. Des. 232, 47–55.
Dix, G.E., 1970. Freon–water modeling of CHF in round tubes. In: ASME Fluid and Heat Transfer Meeting , Detroit, Michigan, USA, Paper No. 70-HT-26.
Fulfs, H., 1980. Comparison of Freon-12 and water steady state CHF data from a PWR 5 × 5-rod bundle. GKSS-Forschungszentrum Geesthacht GmbH, Geesthacht, Germany Report 80/E/29.
Groeneveld, D.C., 1970. Similarity of water and Freon dryout data for uniformly heated tubes. In: ASME Fluid and Heat Transfer Meeting , Detroit, Michigan, USA, Paper No. 70-HT-27.
Green, W.J., Lawther, K.R., 1981. A flow boiling burnout correlation for water and Freon-12. Nucl. Eng. Des. 67, 13–25.
Groeneveld, D.C., Doerffer, S., Tain, R.M., 1997. Fluid-to-fluid modeling of the critical heat flux and post dryout heat transfer. In: Proceedings of the World Congress on Experimental Heat Transfer, Fluid Mechanics and Thermodynamics , Brussels, Belgium, pp. 859–867.
Hou, Y.C., 2000. Experimental investigation on critical heat Flux and post-dryout heat transfer in horizontal helically-coiled tubes. Master Thesis. Xi'an Jiaotong University, Xi'an, China.
Han, J.T., Yu, B., Kang, H.J., Lin, C.X., Ebadian, M.A., 2004. Experimental investigation of condensation heat transfer of R-134a in a helical pipe at three different orientations. J. Refrig. 25, 1–6.
Katto, Y., 1978. A generalized correlation of critical heat flux for the forced convection boiling in vertical uniformly heated round tubes. Int. J. Heat Mass Trans. 21, 1527–1542.
Langhaar, H.L., 1967. Dimensional Analysis and Theory of Models. John Wiley, New York, USA.
Lu, Z.Q., Shi, D.Q., Zhang, Z.J., 1988. Modeling studies on critical heat flux of convective boiling. In: Two-Phase Flow and Heat Transfer. USA Hemisphere Pub. Corp., USA, pp. 207–214.
Lu, Z.Q., 2002. Two-phase Flow and Boiling Heat Transfer. Tsinghua University Press, Beijing, China.
Merilo, M., 1979. Fluid-to-fluid modeling and correlation of flow boiling crisis in horizontal tubes. Int. J. Multiphase Flow 5, 313–325.
Moffat, R.J., 1988. Describing the uncertainties in experimental results. Exp. Therm. Fluid Sci. 1, 3–17.
Pioro, I.L., Cheng, S.C., Groeneveld, D.C., Vasic, A.Z., Pinchon, S., Chen, G., 1999. Experimental study of the effect of non-circular flow geometry on the critical heat flux. Nucl. Eng. Des. 187, 339–362.
Stevens, G.F., Kirby, G.J., 1964. A quantitative comparison between burnout data for water at 1000 psia and Froen-12 at 155 psia, uniformly heated round tubes, vertical upflow. U.K.A.E.A. Report, Winfrith, England, AEEW-R327.
Stevens, G.F., Macbeth, R.V., 1970. The use of Freon-12 to model forced convection burnout in water: the restriction on the size of the model. In: ASME Fluid and Heat Transfer Meeting , Detroit, MI, USA, Paper No.70-HT-20.
Sun, Z.D., 1979. Theory of Dimensional Analysis. The Press Inc. of the People Railway, Beijing, China.
Tain, R.M., Cheng, S.C., Groeneveld, D.C., 1993. Critical heat flux measurements in a round tube for CFCs and CFC alternatives. Int. J. Heat Mass Trans. 36, 2049–3039.

Thome, J.R., 1994. Two-phase heat transfer to new refrigerants. In: Proceeding of 10th International Heat Transfer Conference , Brighton, England, pp. 19–41.
Xin, M.D., Zhou, J., Zhang, G., Chen, Q.H., Cui, W.Z., 2001. R134a boiling in the horizontal tubes with three-dimensional inner microfin. J. Eng. Thermophys. 22, 95–97.
Yang, X.Q., Su, G.H., Gou, J.L., Qiu, H.Z., Jia, D.N., 2005. Theoretical investigation on critical heat flux of annular flow in narrow annular channel. Atomic Energy Sci. Technol. 39, 61–65.
Zhang, Z.J., 1984. Experimental study on fluid to fluid modeling of critical heat flux in flow boiling. Master Thesis. Tsinghua University, Beijing, China.